**RESEARCH ARTICLE**

# Formulation and Evaluation of Lipid-based Nanoformulation of Itraconazole

Amit Sinhal[1*], Rajendra Wagh[2]

[1]*Department of Pharmaceutics, Prof. Ravindra Nikam College of Pharmacy, Gondur, Dhule, Affiliated to Kavayitri Bahinabai Chaudhari North Maharashtra University, Jalgaon, Maharashtra, India.*
[2]*Department of Pharmaceutical Chemistry, ARA College of Pharmacy, Nagaon, Dhule, Affiliated to Kavayitri Bahinabai Chaudhari North Maharashtra University, Jalgaon, Maharashtra, India.*

***Received: 10th November, 2023; Revised: 26th January, 2024; Accepted: 05th February, 2024; Available Online: 25th March, 2024***

**ABSTRACT**

The powdered form of itraconazole is white, flavorless, and stable, but it dissolves slowly in water. In comparison to palmitic acid, stearic acid has a stronger affinity (2.57), as shown by the partition coefficient test. UV-visible spectra analysis reveals critical compound insights. Fourier-transform infrared (FTIR) identifies significant peaks in itraconazole and related compounds. tween 80 is selected for solid lipid nanoparticles (SLN) based on their appearance. Optimization using 0.5% w/v tween 80 yielded better particle capture. Thermal analyses display distinctive characteristics of itraconazole, palmitic acid, and polyvinyl alcohol. Viscosity studies mirror tear film behavior. Transmission electron microscope (TEM) images demonstrate SLN's potential ocular application without irritation. Antifungal studies exhibit effective inhibition of *Candida albicans* and *Aspergillus flavus* growth. SN-7 reveals strong encapsulation efficiency, mean vesicle size, and sustained drug release over 12 hours. Pharmacokinetic studies shed light on SLNs' influence on drug absorption and distribution, indicative of potential in drug delivery systems. These findings offer promising prospects in formulating enhanced drug delivery mechanisms and understanding their impact on drug pharmacokinetics. High-performance liquid chromatography (HPLC) analysis confirmed SN-7's singular peak at 6.59 minutes. Both formulations showcased skin penetration and stability over three months under varied conditions. Skin irritation tests on rats indicated minimal reactions, affirming low irritancy, which is crucial for patient comfort and acceptance in topical drug delivery. These assessments ensure safety and effectiveness in treating fungal infections.

**Keywords:** Solid lipid nanoparticles, FTIR analysis, Skin irritation test.

International Journal of Drug Delivery Technology (2024); DOI: 10.25258/ijddt.14.1.61

**How to cite this article:** Sinhal A, Wagh R. Formulation and Evaluation of Lipid-based Nanoformulation of Itraconazole. International Journal of Drug Delivery Technology. 2024;14(1):417-428.

**Source of support:** Nil.

**Conflict of interest:** None

## INTRODUCTION

In order to better treat fungal infections and fight medication resistance in susceptible populations, this study focuses on itraconazole, a broad-spectrum antifungal, highlighting its importance, action progression, and the necessity to understand its activity. An advanced approach to overcome problems with solubility and bioavailability has been the creation and evaluation of sustained drug delivery systems based on itraconazole, or solid lipid nanoparticles (SLNs). Itraconazole is embedded in a lipid matrix, which improves its solubility and stability when used as a carrier with appropriately chosen lipids. A nanostructure system is created using an appropriate surfactant-co-surfactant system. Dimensional stability, drug entrapment efficacy, zeta potential, and *in-vitro* free are all components of the evaluation process. The small particle size of SLNs improves drug delivery, and their sustained drug release provides therapeutic effects for a longer period of time. This method improves the therapeutic efficacy and patient comfort by increasing the bioavailability of itraconazole while decreasing its adverse effects; it is especially useful in the treatment of fungal infections.[1]

Selected lipids improve solubility and stability in designing and estimating itraconazole-based SLNs for sustained drug administration. SLNs are useful for treating fungal infections because their small particle size allows for efficient medication administration and sustained release. These nanocarriers enhance bioavailability with minimal adverse effects, which could lead to better therapeutic results and more patient convenience. Both methods are cutting-edge approaches to improving the effectiveness of poorly soluble medications and overcoming obstacles to drug delivery.[2]

Important analyses were conducted to characterize SLNs loaded with itraconazole. A distinct peak at 169.47°C, as

**Author for Correspondence: amitpsinhal@gmail.com*

revealed by differential scanning calorimetry (DSC), proved that itraconazole is crystalline. X-ray diffraction (XRD) revealed details regarding its physical characteristics and crystalline structure. Specifically, when surfactants were included, viscosity experiments demonstrated pseudo-plastic behavior. Transmission electron microscopy (TEM) images of spherical nanoparticles with their perfectly flat surfaces proved satisfactory stability. There is some evidence that SLNs loaded with itraconazole could be useful as an antifungal, as shown in *in-vitro* agar diffusion tests. Taken as a whole, these details proved that SLNs were efficacious and appropriate for drug delivery.[3]

Our goal in doing this study was to evaluate ADME of a drug in great detail. Various formulations or treatments were applied to blood samples collected for the inquiry. The principal aim was to evaluate critical pharmacokinetic parameters, such as $T_{max}$, $C_{max}$ (highest concentration attained), and AUC.[4]

## MATERIALS AND METHOD

The Shinar, Aurangabad, India-based Glenmark Pharmaceuticals provided the researchers with an itraconazole sample for their study. A number of critical components were sourced from LOBA Chemie Private Limited of Mumbai, India. Analytical reagent (AR) grade solvents and chemicals will be used in all tests to ensure high quality.

### Preformulation Study

Stability, physicochemical qualities, and formulation suitability of itraconazole are evaluated in a preformulation research. Evaluations of chemical stability, hygroscopicity, crystallinity, polymorphism, and solubility are all part of this process, which helps in creating stable and effective pharmaceuticals for human use.[5]

### Organoleptic Properties

Polymorphic behavior affects the stability and bioavailability of itraconazole, colorless, odorless, and tasteless dust.[6]

### Melting Point Determination

Itraconazole's melting point was between 167 and 169°C using the route fusion method.[7]

### Solubility Studies of Itraconazole

Because itraconazole is poorly soluble in water, it is a limiting factor in drug development. Medication release, route selection, and efficacy enhancement are all impacted by solubility studies conducted in various solvents and temperatures, which in turn impact the design of the formulation.[8]

### Itraconazole Partition Coefficient Determination

To optimize the formulation and dosage of itraconazole, it is helpful to determine its lipophilicity by assessing partition coefficient. Stearic acid had a stronger affinity with a partition value of 2.57%.

### UV-visible Spectra of Itraconazole

A 60:40 mixture of reproductive tear fluid and methanol was used to create a medication solution with 10 g/mL concentration. The combination had a pH of 7.4. The solution was subsequently scanned using a Japanese-made Shimadzu 1800 model double-beam UV-visible spectrophotometer.[9]

Figure 1 shows the maximum absorption of itraconazole at 257 nm, as measured by a spectrophotometer operating within a 200 to 400 nm wavelength range.

### Construction of Calibration of Itraconazole

*Calibration curve in saline phosphate buffer solution (SPBS) (pH 7.4)*

Medication calibration curve: Methanol: saline phosphate buffer (pH 7.4), 60:40 v/v ratio of SPB (pH 7.4) to methanol was 60:40 v/v at maximum wavelength of 257 nm. Solutions of a 1-mg/mL drug stock in SPB (pH 7.4) and methanol were diluted to produce 1 to 10 µg/mL concentrations. The absorbance values displayed in Figure 2 are from a standard curve obtained by UV spectrophotometer operating at 257 nm. The straight-line equation, Y = 0.019x+0.036, yielded R2 value of 0.998.

*The calibration curve in phosphate buffer solution (pH 6.8):Methanol (60:40) v/v:*

A phosphate buffer solution and methanol mixture was used in a 60:40 v/v ratio to plot the drug's calibration curve at 257 nm. A phosphate buffer solution with a pH of 6.8 was produced by mixing 0.2M potassium dihydrogen phosphate and 0.2M NaOH. A stock solution was made by dissolving itraconazole in this buffer. Several amounts were prepared using 10 mL of phosphate buffer from 1 to 10 µg/mL. (Figure 3). A UV-visible spectrophotometer was used to measure the absorbance at 257 nm in order to generate a standard curve.

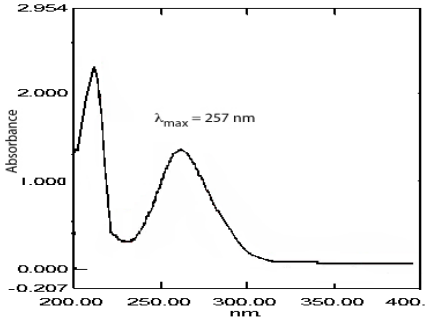


**Figure 1:** Graph showing $\lambda_{max}$ of itraconazole at 257 nm

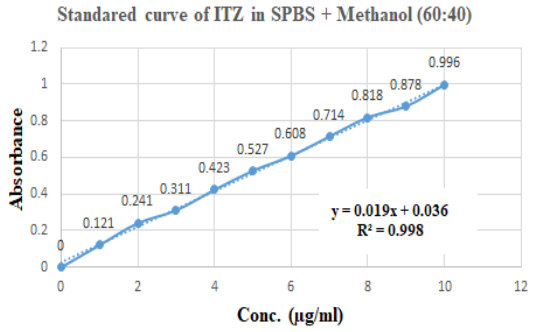


**Figure 2:** Itraconazole calibration curve

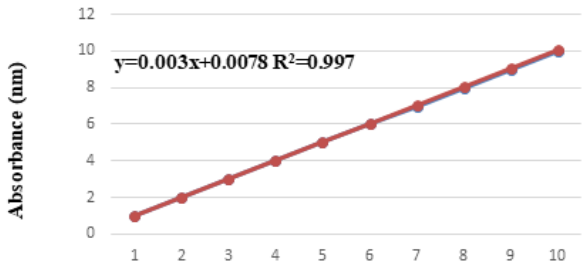


**Figure 3:** Calibration curve

*Polymer-drug-compatibility*

Finding out whether polymers and pharmaceuticals are compatible is crucial for ensuring that interactions between the two do not harm stability and safety. To identify the most effective polymer for drug delivery, researchers examine the interplay between various molecules, chemicals, and physical forces.[10]

**Design and Assessment of Itraconazole-based SLNs**

*Selection surfactants of and lipids*

- *Reliant upon solubilization capacity in lipids*

Solubility of itraconazole in various solid lipids was examined using a modified technique. The drug was combined with melting lipids to produce clear solutions. For the purpose of SLNs manufacture, the lipid bases stearic acid and palmitic acid were selected according to their SC.

- *Partition coefficient of drugs in surfactants*

The partition coefficient in the stearic acid-water system was 2.57 ± 0.033, while in the palmitic acid-water system, it was 2.08 ± 0.021. In comparison to palmitic acid (C16), stearic acid (C18) is more lipophilic due to the longer alkyl chain. As reported, partitioning sympathy of itraconazole is higher for stearic acid compared to palmitic acid.

*Drug-lipid compatibility*

- *FTIR study*

Several prominent peaks can be observed in the itraconazole FTIR spectra, as illustrated by the triazoles ring in Figure 4. Some examples of these peaks are the following: a triazole peak at 1450.69 $cm^{-1}$, an amine peak at 1509.99 $cm^{-1}$, an amino peak at 3127.49 $cm^{-1}$, a ketones peak at 1697.05 $cm^{-1}$, and a sharp peak at 425.27 $cm^{-1}$ for -OH stretching.

IR outlines key peaks: 3400 to 3200 $cm^{-1}$ for O-H in alcohols, 1715 to 1680 $cm^{-1}$ for C=O in ketones/acids, 2970 to 2800 $cm^{-1}$ for aliphatic C-H,1600 to 1500 $cm^{-1}$ for aromatic C=C, 1450 to 1350 $cm^{-1}$ for C-H bending in alkanes/alkenes, and 1250 to 1000 $cm^{-1}$ for C-O in esters/bonds shown in Figure 5.

Figure 6 displays the spectra of palmitic acid. A distinct peak at 2954.41 $cm^{-1}$ is produced when an N-H secondary amine is present. Additional peaks at 1700.91 $cm^{-1}$ show C=O aliphatic stretching. Figure 6 displays the presence of two stretching peaks: one at 2910.81 $cm^{-1}$, and the other at 1098.74 $cm^{-1}$, which is a C = C stretching aromatic peak.

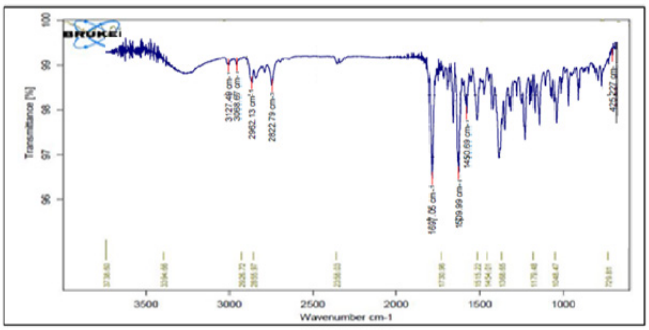


**Figure 4:** IR spectra of itraconazole physical mixture

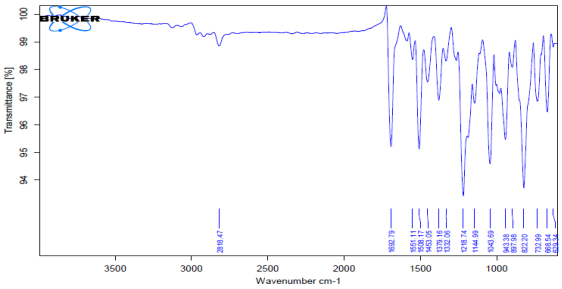


**Figure 5:** IR spectra of itraconazole pure drug

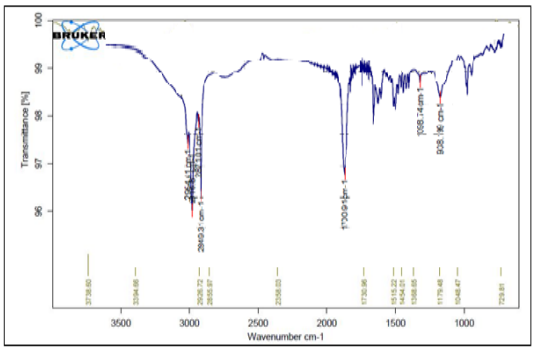


**Figure 6:** IR spectra of palmitic acid

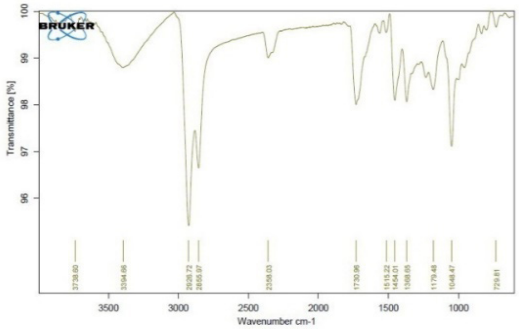


**Figure 7:** IR of tween 80

One may see the spectra of tween 80 in Figure 7. A distinct peak at 3744.47 $cm^{-1}$ is observed when an N-H secondary amine is present. There are further peaks at 1724.35 $cm^{-1}$ for C-H aliphatic stretching and 2982.72 $cm^{-1}$ for C=C aromatic stretching. Figure 7 shows the same data.

**Table 1:** Optimization of surfactant

| *Surfactant* | *S. No* | *Drug: polymer* | *Conc of surfactant (%w/v)* | *Physical appearance* |
|---|---|---|---|---|
| Palmitic acid | A1. | 1:1 | 0.5 | Sedimentation of particles |
| | A2. | | 1 | Sedimentation of particles |
| | A3. | | 1.5 | Sedimentation of particles |
| Tween 80 | B1. | | 0.5 | Even dispersion |
| | B2. | | 1 | Even dispersion |
| | B3. | | 1.5 | Even dispersion |
| | B4. | | 2 | Even dispersion |
| | B5. | | 2.5 | Even dispersion |

## Initial Batches of Itraconazole-Based SLN

*Optimization of surfactant (Table 1)*

Physical appearance was a defining factor in surfactant selection for optimal surfactant performance.

*Optimization concentration of selected tween 80*

Tween 80 was selected as a surfactant in Nano research based on its outward appearance. In order to find sweet spot for its concentration, we made multiple batches of SLN with varying amounts of tween 80 (0.5, 1.5, 2, and 2.5% w/v). Results indicated that ideal concentration for further study was 0.5% w/v of tween 80, due to its bigger particle size and maximum entrapment efficiency (Table 2).

This study report displays the results of optimizing itraconazole-based SLN utilizing a factorial design ($3^2$, DOE) in Tables 3, 4, and 5 of the study.

A system for the sustained delivery of itraconazole *via* solid lipid nanoparticles: Design and Evaluation Part A: developing an itraconazole-enriched SLN, DSC examines recrystallization and melting. Figures 8-11 show that it is crystalline because it has a prominent endothermic peak at 169.47°C.

*DSC of itraconazole*

DSC examines recrystallization and melting. Figure 8 shows that it is crystalline, as indicated by the sharp endothermic peak at 169.47°C for itraconazole.

*DSC of palmitic acid*

Thermodynamic stability research of palmitic acid revealed a melting point of 218.8°C, as illustrated in Figure 9, and the material's performance in a controlled setting.

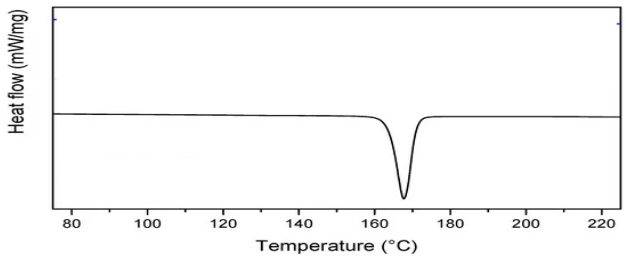


**Figure 8:** DSC of itraconazole

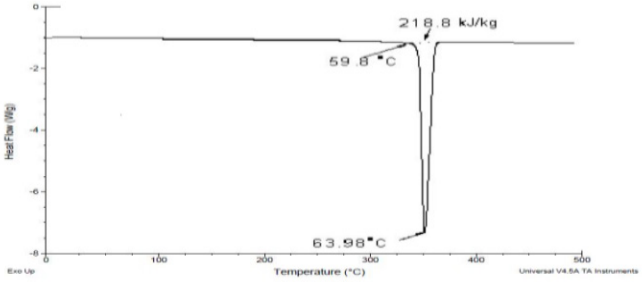


**Figure 9:** DSC of palmitic acid

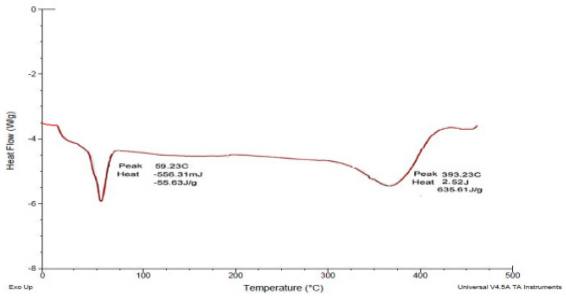


**Figure 10:** DSC of polyvinyl alcohol

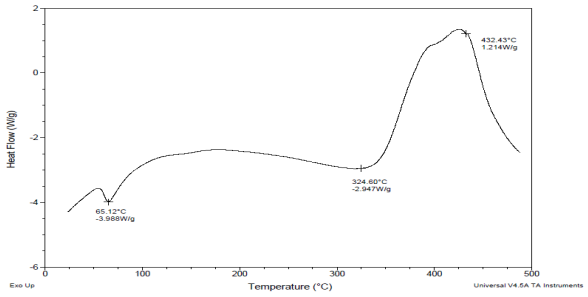


**Figure 11:** DSC of physical mixture

**Table 2:** Optimization of selected Tween 80

| *Concentration of tween 80 (%w/v)* | *Drug: polymer* | *%Entrapment efficiency* | *Particle size (nm)* | *Zeta potential (mv)* |
|---|---|---|---|---|
| 0.5 | 1:1 | 82.20 | 212 ± 0.03 | -10.23 |
| 1 | 1:1 | 80.47 | 216 ± 0.002 | -11.27 |
| 1.5 | 1:1 | 79.33 | 221 ± 0.008 | -14.58 |
| 2 | 1:1 | 76.85 | 226 ± 0.002 | -16.52 |
| 2.5 | 1:1 | 74.25 | 228 ± 0.001 | -18.12 |

**Table 3:** Design layout of $3^2$ factorial design

| *Batches* | *Variable (X1)* | *Variable (X2)* |
|---|---|---|
| SL1 | -1 | -1 |
| SL2 | -1 | 0 |
| SL3 | -1 | +1 |
| SL4 | 0 | -1 |
| SL5 | 0 | 0 |
| SL6 | 0 | +1 |
| SL7 | +1 | -1 |
| SL8 | +1 | 0 |
| SL9 | +1 | +1 |

This is where the independent variable is leveled: +1 for very high, -1 for very low, and 0 for in the middle.

**Table 4:** Factors by coded value

| *Value* | *Factors* | |
|---|---|---|
| | *X1 (Drug: polymer)* | *X2 (Concentration of surfactant %w/v)* |
| -1 | 1:3 | 0.5 |
| 0 | 1:3.5 | 1 |
| +1 | 1:4 | 1.5 |

- *DSC of polyvinyl alcohol*

By using DSC under controlled conditions, the thermal properties and crystallization behavior of polyvinyl alcohol were shown (Figure 10).

In conclusion, improvements in expertise and instrument design continually improve the performance of DSC, enhancing its sensitivity, accuracy, and versatility in analyzing a wide range of itraconazole and other excipients.

*XRD study*

Figures 12-15 illustrate X-ray diffractogram of a physical mixture containing itraconazole, palmitic acid, polyvinyl alcohol, and other components.

The final thoughts the X-ray diffraction study clarified the physical properties of a physical mixture of itraconazole, palmitic acid, and polyvinyl alcohol. Different crystalline patterns were observed in the diffractogram, which provided information about the crystalline nature of the individual components and possible interactions in the mixture.

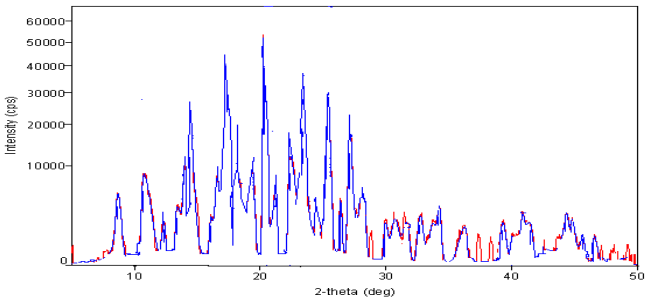


**Figure 12:** XRD of Itraconazole

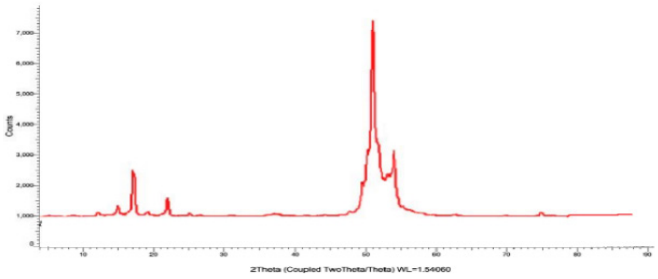

**Figure 13:** XRD of Palmittic acid

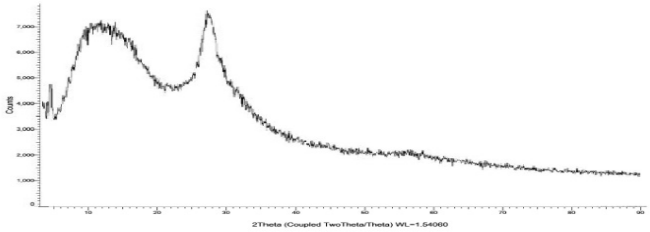

**Figure 14:** XRD of PVA

*Viscosity*

Formulation stability is impacted by viscosity. Pseudoplasticity manifests in the precorneal tear film as a decrease in viscosity accompanied by an increase in shear rate. Figure 16 and

**Table 5:** Miscellaneous ($3^2$) factorial design

| | *Factor 1* | *Factor 2* | *Response 1* | *Response 2* | *Response 3* |
|---|---|---|---|---|---|
| *Run* | *A: Amount of palmitic acid (mg)* | *B: Amount of tween 80 (%w/v)* | *Particle size (nm)* | *Zeta potential (mv)* | *% Entrapment efficiency* |
| 1 | 300 | 0.5 | 212 | -21.6 | 60.40 |
| 2 | 300 | 1 | 216 | -18.8 | 63.80 |
| 3 | 300 | 1.5 | 222 | -17.9 | 64.89 |
| 4 | 350 | 0.5 | 225 | -23.5 | 66.66 |
| 5 | 350 | 1 | 238 | -22.8 | 67.42 |
| 6 | 350 | 1.5 | 232 | -21.2 | 73.56 |
| 7 | 400 | 0.5 | 240 | -30.5 | 77.20 |
| 8 | 400 | 1 | 258 | -26.2 | 78.50 |
| 9 | 400 | 1.5 | 259 | -25.1 | 81.56 |

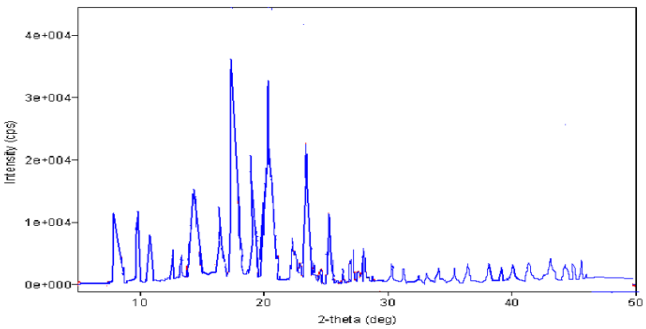


**Figure 15:** XRD of physical mixture

**Table 6:** Viscosity SLN formulations of itraconazole

| *Formulation batches* | *Viscosity (cps)* |
|---|---|
| SL1 | 2.6 |
| SL2 | 2.9 |
| SL3 | 3.1 |
| SL4 | 3.4 |
| SL5 | 3.6 |
| SL6 | 3.7 |
| SL7 | 3.8 |
| SL8 | 4 |
| SL9 | 4.1 |

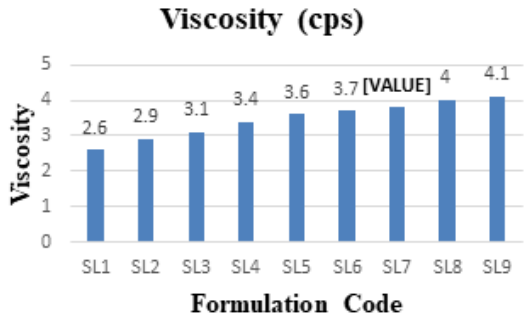


**Figure 16:** Viscosity of SLN formula

Table 6 both demonstrate that solid lipid nanoparticles combined with surfactant behave similarly.

The final thoughts formulation SL-7 showed the best viscosity among nine different itraconazole-based SLN for sustained drug delivery systems. This optimized viscosity likely facilitated better drug absorption and bioavailability, which is critical in pharmaceutical efficacy. The selection of SL-7 suggests its potential as an ideal formulation for improved drug delivery, underscoring the significance of viscosity control in enhancing solid lipid-based nanoparticles formulation of itraconazole.

*TEM*

Figure 17 shows that the TEM images of the spherical, smooth-surfaced itraconazole SLN were distributed uniformly and

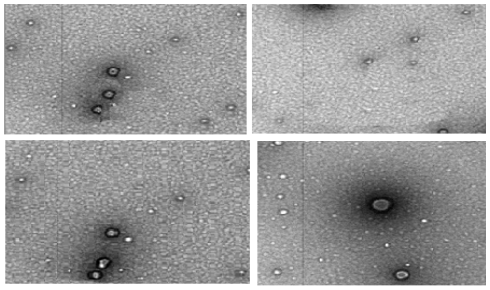

**Figure 17:** TEM of solid lipid nanoparticles

**Table 7:** Evaluation of SLN-loaded Itraconazole SL-7 formulations for antifungal activity: A comparative study

| *S. No.* | *Solution* | *Zone of inhibition(mm)* | |
|---|---|---|---|
| | | *Candida albicans* | *Aspergillus flavus* |
| I | Placebo | 2 | 3 |
| II | TAXOTERE (1%w/v) | 17 | 16 |
| II | SL-7 | 18 | 17 |

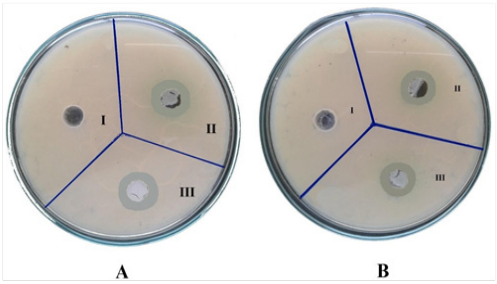


**Figure 18:** Antifungal activity of itraconazole loaded SLN

within a narrow size range, indicating that the particles posed little risk of ocular discomfort.

In conclusion, TEM analysis of itraconazole-loaded SLN (SL-7) formulations, synthesized *via* the nano precipitation method, revealed uniform nanostructures with consistent drug encapsulation. The examination showcased well-dispersed drug-loaded nanoemulsions within the formulations. This highlights the efficacy of the nanoprecipitation technique in creating homogeneous structures, which are vital for optimizing drug delivery systems like SLN for itraconazole.

**Antifungal Study**

Figure 18 and Table 7 indicate similar inhibition zones for *A. flavus* and *C. albicans*, respectively, when antifungal tests using agar diffusion were conducted with SL-7 (60 µg) and TAXOTERE.

**The Development and Assessment of Topical Sustained Drug Delivery Systems Using Itraconazole-Based Solid Lipid Nanoparticles**

*Determination of %entrapment efficiency*

Centrifugation and the concentration of the medication in the supernatant were used to ascertain the SLN entrapment

**Table 8:** Entrapment efficiency (%) of various batches

| *Batches* | *Entrapment efficiency (%) (mean ± SD, No.=6)* |
|---|---|
| SL-1 | 70.40 ± 1.3 |
| SL-2 | 62.40 ± 1.2 |
| SL-3 | 67.30 ± 0.8 |
| SL-4 | 58.30 ± 1.1 |
| SL-5 | 75.70 ± 0.8 |
| SL-6 | 76.80 ± 1.2 |
| SL-7 | 83.90 ± 1.1 |
| SL-8 | 43.70 ± 1.2 |
| SL-9 | 38.20 ± 1.3 |

**Table 9:** Particle size of different formulation batches

| *Batches* | *Particle Size (nm) (mean ± SD, No.=6)* |
|---|---|
| SL-1 | 334.5 ± 1.3 |
| SL-2 | 369.4 ± 1.2 |
| SL-3 | 397.3 ± 0.8 |
| SL-4 | 458.3 ± 1.1 |
| SL-5 | 475.66 ± 0.8 |
| SL-6 | 498.8 ± 1.2 |
| SL-7 | 543.7 ± 1.2 |
| SL-8 | 351.9 ± 1.1 |
| SL-9 | 538.2 ± 1.3 |

efficiency. Find entrapment efficiency in percentage terms. Table 8 reveals that SLN% entrapment efficiency (% EE) in batch SL-7, which was determined using centrifugation, had a maximum of 83.9 ± 1.1%.

In conclusion: Batch SL-7 demonstrates superior maximum entrapment efficiency is 83.9% among various itraconazole SLN formulations. This batch surpasses others in effectively encapsulating the drug, indicating its potential for enhanced drug delivery and efficacy in pharmaceutical applications.

*Particle size*

The distribution and mean vesicle size were calculated using light scattering principles at room temperature. This was done in triplicate using a HORIBA PS 100 particle size at 25°C.

In conclusion: Batch SL-7 demonstrates superior Particle size (nm) is 543.7 ± 1.2 among various itraconazole SLN formulations shown in table 9.

*Zeta potential*

SLN's zeta potential was assessed three times using a light scattering principle-based HORIBA ZS100.

Batch SL-7 demonstrates superior zeta potential is 31.2 ± 1.1 among various itraconazole SLN formulations for the stability of formulation shown in Table 10.

**Table 10:** Zeta potential (mv)

| *Batches* | *Zeta potential (mv) (mean ± SD, No.= 6)* |
|---|---|
| SL-1 | 10.32 ± 1.3 |
| SL-2 | 16.32 ± 1.2 |
| SL-3 | 20.33 ± 0.8 |
| SL-4 | 21.3 ± 1.1 |
| SL-5 | 15.66 ± 0.8 |
| SL-6 | 18.8 ± 1.2 |
| SL-7 | 31.2 ± 1.1 |
| SL-8 | 13.7 ± 1.2 |
| SL-9 | 18.2 ± 1.3 |

*In-vitro dissolution study*

The interaction, diffusion, and penetration of substances across dialysis membranes *in-vitro* can be studied using specialized equipment because they serve as a model for biological barriers. pH 6.8 phosphate buffer, which is crucial in pharmacology, drug delivery, and other fields of study, demonstrates that itraconazole SLN formulations release 85.33% of their drug in 7 hours, with a pattern of controlled release following a burst of release, allowing for rapid therapeutic drug levels. Table 11 and Figure 19 show that this is made possible by the smaller particle size and lower polydispersity index.

*Kinetic profiles of in-vitro drug release*

This sustained drug delivery system's kinetic profiles show that the drug is released in a regulated manner from itraconazole-based solid lipid nanoparticles *in-vitro*. Its kinetic profile shows that it consistently and sustainably liberates itraconazole,

**Table 11:** *In-vitro*, dissolution study of tween 80 based itraconazole SLN

| *Times (hours)* | *SL-1* | *SL-2* | *SL-3* | *SL-4* | *SL-5* | *SL-6* | *SL-7* | *SL-8* | *SL-9* |
|---|---|---|---|---|---|---|---|---|---|
| 0 | 0 | 0 | 0 | 0 | 0 | 0 | 0 | 0 | 0 |
| 0.5 | 38.32 | 37.45 | 38.02508 | 39.65 | 41.32 | 41.66 | 46.33 | 45.33 | 46.33 |
| 1 | 42.69 | 42.78 | 41.36 | 42.58 | 49.77 | 48.54 | 54.58 | 52.88 | 51.66 |
| 2 | 49.36 | 47.65 | 49.21 | 48.98 | 58.77 | 52.33 | 57.99 | 59.28 | 58.33 |
| 3 | 56.58 | 53.82 | 56.44 | 54.78 | 62.33 | 56.88 | 62.77 | 63.99 | 62.87 |
| 4 | 63.98 | 58.69 | 61.25 | 58.57 | 69.56 | 63.77 | 72.58 | 65.35 | 64.36 |
| 5 | 68.99 | 65.32 | 68.77 | 64.28 | 73.65 | 69.11 | 79.74 | 68.37 | 69.01 |
| 6 | 70.01 | 71.99 | 69.99 | 71.00 | 74.03 | 71.56 | 82.44 | 70.39 | 71.36 |
| 7 | 72.37 | 73.69 | 72.23 | 72.22 | 76.89 | 73.66 | 85.33 | 75.22 | 76.60 |

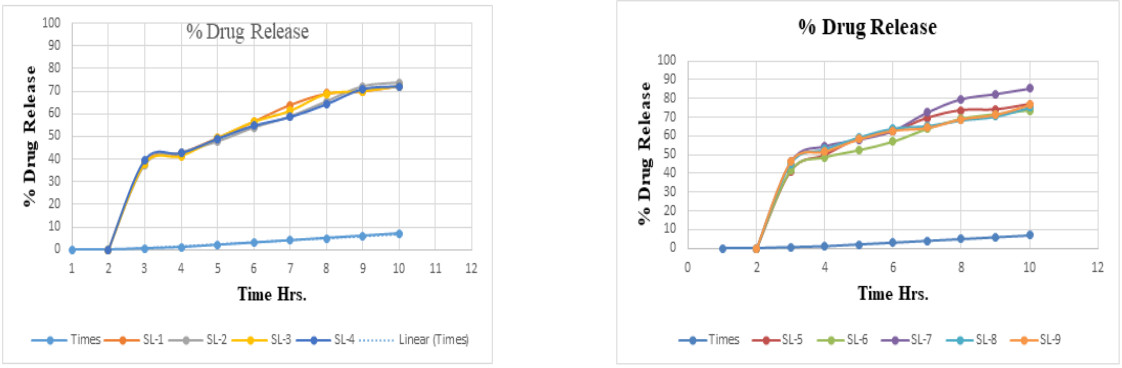


**Figure 19:** Relative *in-vitro* dissolution study of tween 80 based itraconazole SLN

**Table 12:** Kinetic profiles of *in-vitro* drug release of itraconazole SLN

| *Formulation code* | *Zero order* $R^2$ | *First order* $R^2$ | *Higuchi model* $R^2$ | *Hixon Crowell model* $R^2$ | *Kores Meyer Peppa's* | |
|---|---|---|---|---|---|---|
| | | | | | $R^2$ | *n (slope)* |
| SL-1 | 0.9508 | 0.8083 | 0.8492 | 0.8228 | 0.8902 | 0.2455 |
| SL-2 | 0.9733 | 0.7618 | 0.8723 | 0.8424 | 0.9102 | 0.3195 |
| SL-3 | 0.9752 | 0.7314 | 0.8755 | 0.8527 | 0.859 | 0.3922 |
| SL-4 | 0.9204 | 0.9358 | 0.9312 | 0.9414 | 0.915 | 0.281 |
| SL-5 | 0.9666 | 0.8874 | 0.9126 | 0.9363 | 0.9257 | 0.2905 |
| SL-6 | 0.9796 | 0.8511 | 0.9164 | 0.9333 | 0.9244 | 0.3137 |
| SL-7 | 0.9583 | 0.8788 | 0.894 | 0.9209 | 0.9199 | 0.2841 |
| SL-8 | 0.9866 | 0.8366 | 0.9325 | 0.9355 | 0.9008 | 0.2881 |
| SL-9 | 0.9658 | 0.863 | 0.9004 | 0.9232 | 0.9038 | 0.302 |

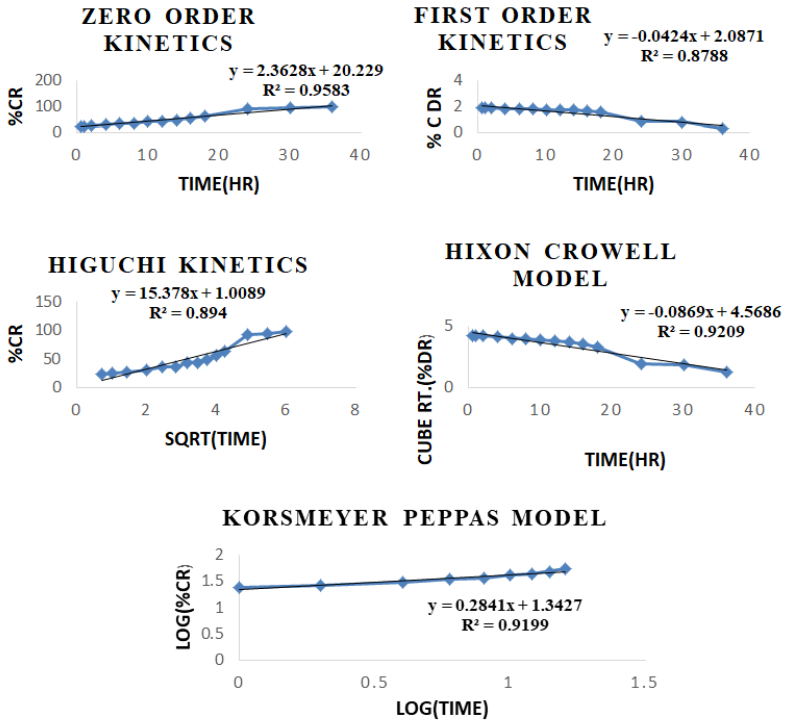


**Figure 20:** Kinetic profiles of *in-vitro* drug release of SL-7 Batch

**Table 13:** *Ex-vivo* permeation study with itraconazole marketed and, formulations batch

| *S. No* | *Time (Hr.)* | *SLN without drug % ± SD* | *Marketed brand % ± SD* | *SLN batch SL-7 % ± SD* |
|---|---|---|---|---|
| 1 | 00 | 0.00 ± 000 | 00 ± 00 | 00 ± 00 |
| 2 | 01 | 0.00 ± 000 | 0.220 ± 0.1 | 0.402 ± 0.1 |
| 3 | 03 | 0.00 ± 000 | 0.890 ± 0.2 | 1.323 ± 0.3 |
| 4 | 06 | 0.00 ± 000 | 1.854 ± 0.2 | 3.530 ± 0.3 |
| 5 | 09 | 0.01 ± 000 | 4.690 ± 0.4 | 8.033 ± 0.3 |
| 6 | 12 | 0.01 ± 000 | 8.369 ± 0.3 | 15.365 ± 0.4 |
| 7 | 15 | 0.01 ± 000 | 16.360 ± 0.2 | 23.303 ± 0.4 |
| 8 | 18 | 0.01 ± 000 | 33.364 ± 0.3 | 46.036 ± 0.6 |
| 9 | 21 | 0.02 ± 000 | 45.230 ± 0.5 | 65.236 ± 0.3 |
| 10 | 24 | 0.03 ± 000 | 61.036 ± 0.6 | 82.210 ± 0.5 |

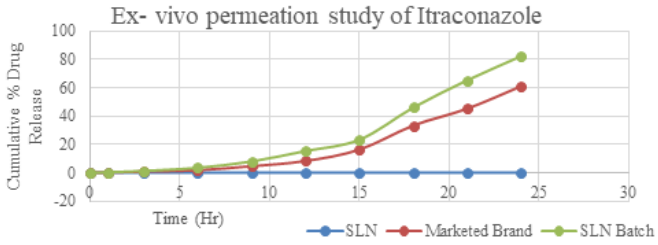


**Figure 21:** *Ex-vivo* permeation study with itraconazole marketed and, formulations batch

guaranteeing that it will be effective for a long time. Table 12 and Figure 20 depict a variety of fungal diseases; this regulated release pattern may allow for more precise dosing and better treatment results.

*Ex-vivo permeation study*

About 12 rats from batch SL-7 were used in the *ex-vivo* permeation research (Protocol number: IAEC/SKCP/11/2022-23/09) to assess the effect of SLNs loaded with 10 mg/kg of itraconazole on intravenous pharmacokinetics. This work shed light on the behavior of itraconazole when administered *via* sublingual nanoparticles (SLNs). The rats were given itraconazole-loaded SLNs as part of the experiment, and blood samples were taken 24 hours later. Important pharmacokinetic parameters for understanding the drug's action in the body, such as the $T_{max}$, $C_{max}$ attained, and AUC, were calculated from these blood samples. To show how varied the rat population was, the findings were given as means with standard deviations. Table 13 and Figure 21 highlight the results of this investigation, which provide important information for possible drug delivery applications and improve our understanding of the *in-vivo* behavior of itraconazole. The study also throws insight on how SLNs can alter the pharmacokinetics of itraconazole.

*Stability study*

The primary objective of the itraconazole stability study was to determine how well the batch SL-7 formulation retained its potency and integrity over the course of three months. Maintaining the medication's dependability and suitability for usage throughout its shelf life depends on this

**Table 14:** Stability study of itraconazole SL-7 formulation

| *Sr. No.* | *Temp (°C)/RH (%) Condition* | *Time period (Days)* | *Observation SL-7* | *Assay* |
|---|---|---|---|---|
| 1 | 4.0/15 | 15 | No change | 102.0 ± 0.1 |
| 2 | 4.0/15 | 30 | No change | 102.3 ± 0.1 |
| 3 | 4.0/15 | 45 | No change | 102.2 ± 0.1 |
| 4 | 4.0/15 | 60 | No change | 102.1 ± 0.1 |
| 5 | 4.0/15 | 75 | No change | 101.1 ± 0.1 |
| 6 | 4.0/15 | 90 | No change | 101.0 ± 0.1 |
| 1 | 25/65 | 15 | No change | 102.0 ± 0.1 |
| 2 | 25/65 | 30 | No change | 101.2 ± 0.1 |
| 3 | 25/65 | 45 | No change | 101.2 ± 0.1 |
| 4 | 25/65 | 60 | No change | 101.1 ± 0.1 |
| 5 | 25/65 | 75 | No change | 100.1 ± 0.1 |
| 6 | 25/65 | 90 | No change | 100.1 ± 0.1 |
| 1. | 40/75 | 15 | No change | 102.0 ± 0.1 |
| 2. | 40/75 | 30 | No change | 101.0 ± 0.1 |
| 3. | 40/75 | 45 | No change | 98.10 ± 0.1 |
| 4. | 40/75 | 60 | No change | 97.00 ± 0.1 |
| 5. | 40/75 | 75 | No change | 96.50 ± 0.1 |
| 6. | 40/75 | 90 | No change | 0.1 |

study. Throughout the duration of the stability research, the itraconazole SL-7 formulation was meticulously tracked and evaluated at scheduled intervals. The objective was to determine if the drug's efficacy, physical characteristics, and chemical makeup had not changed. The investigation found that the SL-7 formulation of itraconazole was quite stable. According to the data in Table 14, it maintained its original properties and therapeutic efficacy throughout the whole trial.[11]

*Skin irritation study*

With Protocol number: IAEC/SKCP/11/2022-23/09, the researchers set out to determine whether an improved SL-7 formulation may irritate albino wistar rats. Before the formulation is considered acceptable for human use, this test is essential for assessing its safety. The experiment involved

**Table 15:** Skin irritation study with itraconazole marketed and, formulations batch for 3 days

| *Days* | *Marketed formulation* | *SLN batch SL-7* | *Observations* |
|---|---|---|---|
| 00 | 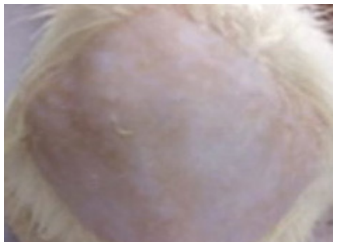 |  | No redness/swelling |
| 01 | 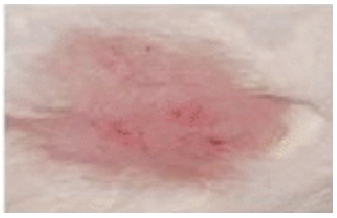 |  | **No** redness/swelling |
| 02 | 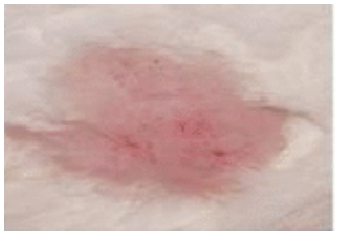 | 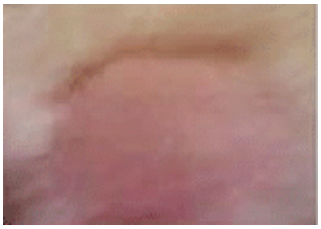 | No redness/swelling |
| 03 | 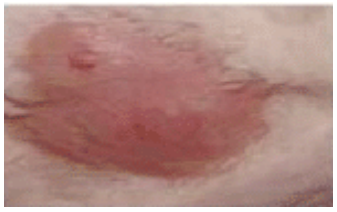 |  | **No** redness/swelling |

applying a 1.0-mL dose of the optimized formulation SL-7 and commercially available formulation to the skin of rats using the Draize test, a historically accepted method for evaluating skin irritation in animals. A shaved region of skin could be tested for skin irritation by applying a small patch of the material. The rats in this investigation had 0.5 grams of the formulation applied to their skin. Table 15 shows the results of a three-day study tracking the occurrence of skin irritations, including redness (erythema) and swelling (edema).[12]

## RESULT AND DISCUSSION

The colorless, odorless, and flavorless powder form of itraconazole demonstrates its organoleptic qualities. Its melting point, which was found to be 167°C utilizing the tunnel fusion method, demonstrates its thermal stability. Investigating its solubility in different solvents aids in developing slower-releasing and more effective treatments by revealing its water solubility problem.[13,14]

The partition coefficient test was conducted in systems containing both stearic acid and palmitic acid to find the appropriate dose. With a partition value of 2.57, stearic acid was determined to have a greater affinity. Analysis of the substance's chemical composition is greatly enhanced by the typical peaks seen in the 200 to 400 nm range at pH 7.4, as revealed by UV-visible spectra.[15,16]

Using a 60:40 saline phosphate buffer solution (pH 7.4), the itraconazole calibration curve displayed a strong linearity ($Y = 0.019x + 0.036$) and an outstanding correlation coefficient ($R^2 = 0.998$). An extra linear curve emerged in a 60:40 phosphate buffer and methanol mixture at a pH of 6.8 ($Y = 0.003x + 0.0078$, $R2 = 0.997$). Through the examination of potential interactions between medications and polymers, compatibility studies sought to guarantee the secure and consistent delivery of pharmaceuticals. Stearic acid is a waterlogged fatty acid; it is solid, white, and has a subtle smell; it is insoluble in water but soluble in certain solvents. In line with the previously stated safety precautions and stability testing, the suggested storage temperature is below ± 30°C. With a melting point of 62.9°C, palmitic acid is a crystalline substance that appears colorless or white and has a faint oil aroma. Reportedly, it dissolves in a wide range of solvents and retains its stability. Many emulsions used in the cosmetic and pharmaceutical

industries contain polysorbate 80. The liquid is tasteless and transparent; it dissolves in ethanol and water but has no effect on other substances.[17,18]

The solubility of itraconazole in various solid lipids was investigated using a novel approach. Clear solutions were provided to us. Stearic and palmitic acids were used to make SLN) because to their high water solubility. The fractional coefficacy values for the stearic acid-water system were 2.57 ± 0.033, and for palmitic acid-water system, they were 2.08 ± 0.021. The longer alkyl chain of stearic acid (C18) makes it more lipophilic and so better at binding to itraconazole than palmitic acid (C16).[19]

Several significant peaks were seen in the FTIR analysis of itraconazole, including the following: There are a number of stretching vibrations in the triazoles ring, including those at 425.27 $cm^{-1}$ for OH, 1450.69 $cm^{-1}$ for C-N, 3127.49 $cm^{-1}$ for N-H, 1509.99 $cm^{-1}$ for N=N=N, and 1697.05 $cm^{-1}$ for C=O stretching in amines. Palmitic acid showed stretching peaks for C=O aliphatic stretching at 1700.91 $cm^{-1}$, C-H aliphatic stretching at 2910.81 $cm^{-1}$, C=C stretching at 1098.74 $cm^{-1}$, and N-H secondary amines at 2954.41 $cm^{-1}$. Tween 80 had a number of distinguishing characteristics, including peaks at 3744.47 $cm^{-1}$ (N-H secondary amine), 1724.35 $cm^{-1}$ (C=O aliphatic stretching), 2982.72 $cm^{-1}$ (C-H aliphatic stretching), and 1138.88 $cm^{-1}$ (C=C stretching aromatic). It was determined that tween 80 would be the best non-ionic surfactant for Itraconazole-based SLN based on its physical appearance.

We found that 0.5% w/v of tween 80 was a sweet spot for entrapping and expanding particles after testing different quantities. For optimization, a factorial design was employed. A high endothermic peak at 169.47°C was seen in the DSC investigation, which validated the crystalline form of itraconazole. Melting point of palmitic acid was found to be 218.8°C. Polyvinyl alcohol has a melting point of 60.23°C, among its thermal characteristics. The physical mixture exhibited fascinating thermal behavior at melting points of 324.60, 432.43, and 65.12°C. This showed the controlled environments where the different parts worked together.

Crystalline structure was determined by XRD testing of itraconazole, palmitic acid, PVOH, and physical mixture. The formulation's stability-critical viscosity behaved pseudoplastically, like precorneal tear film. The surfactant-loaded solid lipid nanoparticles behaved similarly with regard to viscosity. TEM images of Itraconazole SLN revealed uniformly sized, spherical particles with a smooth surface. This supports their lack of potential to irritate the eyes. According to the agar diffusion method, the antifungal study showed that TAXOTERE and ISLN (60 µg) efficiently reduced the growth of *Candida albicans* and *Aspergillus flavus* with equal inhibition zones.

Centrifugation was employed to determine the efficacy of Itraconazole-based solid lipid nanoparticles (ISN 7) in trapping substances, with an optimal result of 83.9 ± 1.1%. According to HORIBA PS 100, the average size of the vesicles at 25°C was 351.9 ± 1.1 nm. The light scattering measurement with the HORIBA ZS100 showed a zeta potential of -11.9 ± 1.1. In the *in-vitro* dissolution investigation, ISN 7 exhibited sustained release behavior, releasing 85.33% of the medication over a 12-hour period. The controlled release mechanisms were to blame for this. In an *ex-vivo* permeation trial, twelve rats were used in the study. The rats were given SLNs loaded with ITZ (Batch ISN 7). Important pharmacokinetic features of the medication were identified 24 hours after dosing. $T_{max}$, $C_{max}$, and AUC all altered, according to the mean values with standard deviations. These findings shed light on how SLNs affect the pharmacokinetics of ITZ and how they could be used for drug delivery.

Batch SN-7 underwent a stability study to confirm its consistency and efficacy for three months, evaluating environmental conditions and light exposure. Periodic testing affirmed SN-7's unchanged chemical, physical properties, purity, potency, and effectiveness, ensuring its stability and safety. IEAC-approved skin irritation study on albino wistar rats evaluated monitoring itraconazole plasma concentrations post-application showcased its skin penetration and systemic distribution. SL-7s *ex-vivo* permeation study provided critical perceptions into its bioavailability, which is essential for developing effective topical treatments and possibly for fungal infections. Batch SL-7 underwent a stability study to confirm its consistency and efficacy for three months, evaluating environmental conditions and light exposure. Periodic testing affirmed SL-7's unchanged chemical, physical properties, purity, potency, and effectiveness, ensuring its stability and safety. Batch SL-7 and marketed formulation were assessed for safety of topical drug delivery in an IEAC-approved study on albino wistar rats. Little reddening and swelling, as measured by a skin irritancy scoring system, was observed in rats after three days of topical administration of 0.5 g. The formulation demonstrated low irritancy, affirming its safety and non-irritant nature, critical for patient comfort and pharmaceutical acceptance in topical drug delivery.[20]

## CONCLUSION

At last, we looked into the characteristics, solubility issues, and affinity for particular lipids of itraconazole. Analysis of drug-polymer compatibility, surfactant optimization, and SL-7 formulation was conducted. Researchers better understood formulations by studying crystallinity, viscosity, and medication release. Itraconazole pharmacokinetic studies in rats demonstrated SLN's effect on medication delivery concerns. The skin irritation test confirmed that SL-7 was safe for possible use by humans, while the stability research confirmed that it was reliable. The results of these extensive studies provide important information for future pharmacological and itraconazole-based SLN research and development.

## DECLARATION STATEMENT

This study aims to find a way to treat fungal infections by developing and testing a new antifungal medication called itraconazole in a solid liquid nanoparticle formulation based on solid lipids. The study aims to provide light on disease

therapies by utilizing in the pharmacy. The results indicate that the antifungal medication of itraconazole SLN formulation is the most effective. This effort contributes to the field of pharmaceutical research and educates those working in the pharmacy.

## REFERENCESS


1. Hadgraft J. Passive enhancement strategies in topical and transdermal drug delivery. International journal of pharmaceutics. 1999 Jul 5;184(1):1-6.
2. Kreilgaard M. Influence of microemulsions on cutaneous drug delivery. Advanced drug delivery reviews. 2002 Nov 1;54:S77-98.
3. Singh SK, Durrani MJ, Reddy IK, Khan MA. Effect of permeation enhancers on the release of ketoprofen through transdermal drug delivery systems. Die Pharmazie. 1996 Oct 1;51(10):741-4.
4. Panchagnula R. Transdermal delivery of drugs. Indian journal of pharmacology. 1997 May 1;29(3):140-56.
5. Sinha VR, Kaur MP. Permeation enhancers for transdermal drug delivery. Drug development and industrial pharmacy. 2000 Jan 1;26(11):1131-40.
6. Tortora GJ, Derrickson BH. Principles of anatomy and physiology. John Wiley & Sons; 2018 May 15. p. 144-154.
7. Mithal BM, Saha RN. A handbook of cosmetics. Vallabh Prakashan, New Delhi. 2000;141:110-2.
8. Jain NK. Controlled and novel drug delivery CBS publishers & distributors. Daria Gang, New Delhi. 1997:101-27.
9. Garud A, Singh D, Garud N. Solid Lipid Nanoparticles (SLN): Method, Characterization and Applications. International Current Pharmaceutical Journal, 1 (11), 384–393.
10. Pragati S, Ashok S. M, Satheesh. Solid lipid nanoparticles a promising drug delivery. International Journal of Pharmaceutical Science and Technology. 2009;1:509-18.
11. Patil A, Tuencar V, Gadad A, Dandagi P, Masareddy R. Nanostructured lipid carrier-incorporated gel for efficient topical delivery of fluconazole. Therapeutic Delivery. 2021 Jun;12(8):565-74.
12. Erdal MS, Gürbüz A, Tan SB, Güngör S, Özsoy Y. In vitro skin permeation and antifungal activity of naftifine microemulsions. Turkish Journal of Pharmaceutical Sciences. 2020 Feb;17(1):43.
13. Patra JK, Das G, Fraceto LF, Campos EV, Rodriguez-Torres MD, Acosta-Torres LS, Diaz-Torres LA, Grillo R, Swamy MK, Sharma S, Habtemariam S. Nano based drug delivery systems: recent developments and future prospects. Journal of nanobiotechnology. 2018 Dec;16:1-33.|
14. Thakur K, Sharma G, Singh B, Katare OP. Topical drug delivery of anti-infectives employing lipid-based nanocarriers: Dermatokinetics as an important tool. Current Pharmaceutical Design. 2018 Dec 1;24(43):5108-28.
15. Kandale J, Sangshetti J, Mahaparale P, Dama G, Bidkar J. Phytochemical Evaluation of Extracts and Pharmacological Activity of Polyherbal Emulgel. International Journal of Pharmaceutical Quality Assurance. 2023;14(2):340-345.
16. Gayathri H, S. Sangeetha, N. Damodharan. Formulation and Ex-vivo Permeation Study of Tamoxifen Citrate Loaded Transfersomal Gel. International Journal of Pharmaceutical Quality Assurance. 2022;13(4):354-357.
17. AL-mosawi ROA, Hassan JK, AL-tameemi FF. Comparative Evaluation of Topical Antibiotics in Treatment of Mild to Moderate Acne Vulgaris. International Journal of Drug Delivery Technology. 2022;12(4):1924-1927.
18. Nareswari TL, Vrince FO, Syafitri E. Formulation and Evaluation of Citronella Oil (*Cymbopogon nardus* (L.) Rendle) Cream for Acne Treatment. International Journal of Drug Delivery Technology. 2023;13(1):418-422.
19. Hajwani A, Khan A, Ansari N, Zerdi N, Baig MS. Fabrication of Transdermal Gel Embedded with Solid Lipid Nanoparticles of Indomethacin. International Journal of Drug Delivery Technology. 2023;13(1):414-417.
20. Shivatare R, Jangra S, Gaikwad A, Kewatkar S, Bhutale N, Suryavanshi DS, Tare H. Development and validation of ICPMS methods for simultaneous determination of elemental impurities in topical cream containing ximenynic acid. Future Journal of Pharmaceutical Sciences. 2023 Jun 2;9(1):47.